REPORT DOCUMENTATION PAGE

Form Approved
OMB No. 0704-0188

1. REPORT DATE *(DD-MM-YYYY)*	2. REPORT TYPE	3. DATES COVERED *(From - To)*
03-06-2007	Technical Paper	

4. TITLE AND SUBTITLE

Dependence of Electron Peak Current on Hollow Cathode Dimensions and Seed Electron Energy in a Pseudospark Discharge (Preprint)

5a. CONTRACT NUMBER
FA8650-04-C-2511

5b. GRANT NUMBER

5c. PROGRAM ELEMENT NUMBER

6. AUTHOR(S)
S.O. Cetiner, P. Stoltz, & P. Messmer (Tech-X Corp.); Jean-Luc Cambier (AFRL/PRSA)

5d. PROJECT NUMBER

5e. TASK NUMBER
OSDBR4QP

5f. WORK UNIT NUMBER

7. PERFORMING ORGANIZATION NAME(S) AND ADDRESS(ES)

Tech-X Corporation
5641 Arapaohe Avenue, Suite A
Boulder CO 83030

8. PERFORMING ORGANIZATION REPORT NUMBER

AFRL-PR-ED-TP-2007-324

9. SPONSORING / MONITORING AGENCY NAME(S) AND ADDRESS(ES)

Air Force Research Laboratory (AFMC)
AFRL/PRS
5 Pollux Drive
Edwards AFB CA 93524-7048

10. SPONSOR/MONITOR'S ACRONYM(S)

11. SPONSOR/MONITOR'S NUMBER(S)
AFRL-PR-ED-TP-2007-324

12. DISTRIBUTION / AVAILABILITY STATEMENT

Approved for public release; distribution unlimited (PA #07236A).

13. SUPPLEMENTARY NOTES
For publication in the *Journal of Applied Physics*.

14. ABSTRACT

The pre-breakdown and breakdown phases of a pseudospark discharge are investigated using the two-dimensional kinetic plasma simulation code OOPIC™ Pro. Trends in the peak electron current at the anode are presented as function of the hollow cathode dimensions and mean seed injection velocities at the cavity back wall. The plasma generation process by ionizing collisions is examined, showing the effect on supplying the electrons that determine the density of the beam. The mean seed velocities used here are varied between the velocity corresponding to the energy of peak ionization cross-section, fifteen times this value and no mean velocity (i.e. electrons injected with a temperature of 2.5 eV). The reliance of the discharge characteristics on the penetrating electric field is shown to decrease as the mean seed injection velocity increases because of its ability to generate a surplus plasma independent of the virtual anode. As a result, the peak current increases with the hollow cathode dimensions for the largest average injection velocity, while for the smallest value it increases with the area of penetration of the electric field in the hollow cathode interior. Additionally, for a given geometry an increase in the peak current with the surplus plasma generated is observed. Although the present study uses Argon only, the variation in the discharge dependencies with the seed injection energy relative to the ionization threshold is expected to apply independently of the gas type. Secondary electrons due to electron and ion impact are shown to be important only for the largest impact areas and discharge development times of the study.

15. SUBJECT TERMS

16. SECURITY CLASSIFICATION OF:			17. LIMITATION OF ABSTRACT	18. NUMBER OF PAGES	19a. NAME OF RESPONSIBLE PERSON
					Dr. Jean-Luc Cambier
a. REPORT	b. ABSTRACT	c. THIS PAGE	SAR	25	19b. TELEPHONE NUMBER *(include area code)*
Unclassified	**Unclassified**	**Unclassified**			N/A

Standard Form 298 (Rev. 8-98)
Prescribed by ANSI Std. 239.18

Dependence of Electron Peak Current on Hollow Cathode Dimensions and Seed Electron Energy in a Pseudospark Discharge (Preprint)

S. O. Cetiner, P. Stoltz and P. Messmer

Tech-X Corp., 5641 Arapaohe Ave., Suite A, Boulder, CO 83030

J.-L. Cambier

Air Force Research Laboratory, AFRL/PRSA, Edwards AFB, CA 93524

The pre-breakdown and breakdown phases of a pseudospark discharge are investigated using the two-dimensional kinetic plasma simulation code OOPIC™ Pro. Trends in the peak electron current at the anode are presented as function of the hollow cathode dimensions and mean seed injection velocities at the cavity back wall. The plasma generation process by ionizing collisions is examined, showing the effect on supplying the electrons that determine the density of the beam. The mean seed velocities used here are varied between the velocity corresponding to the energy of peak ionization cross-section, fifteen times this value and no mean velocity (i.e. electrons injected with a temperature of 2.5 eV). The reliance of the discharge characteristics on the penetrating electric field is shown to decrease as the mean seed injection velocity increases because of its ability to generate a surplus plasma independent of the virtual anode. As a result, the peak current increases with the hollow cathode dimensions for the largest average injection velocity, while for the smallest value it increases with the area of penetration of the electric field in the hollow cathode interior. Additionally, for a given geometry an increase in the peak current with the surplus plasma generated is observed. Although the present study uses Argon only, the variation in the discharge dependencies with the seed injection energy relative to the ionization threshold is expected to apply independently of the gas type. Secondary electrons due to electron and ion impact are shown to be important only for the largest impact areas and discharge development times of the study.

I. INTRODUCTION

The pseudospark is a low pressure transient gas discharge with a particular geometrical configuration[1-4] capable of producing a rapid current rise up to 10^{12} A/s [1] and generating current densities[4] $>10^6$ A/cm^2 . The pseudospark has found applications in fast high power switching[4] as well as X-ray[5,6], laser radiation and microwave generation[6], while the electron beam produced during the triggering phase is also of interest in materials processing and thin film production[5]. The pseudospark is generally composed of hollow electrodes, generally cylindrical, with a hole on the axis, typically a few millimeters in radius, separated by an insulator. In some configurations, the anode is planar, and may also have a hole aligned with that of the cathode (e.g. for electron beam propagation). The approximate dimensions[5] in a standard sized pseudospark include a diameter in the range 3 to 6 cm and a length of 3 to 7.5 cm. Scaling down of the pseudospark to a "compact" size has been achieved[7], where the cavity radius is less than a centimeter and the total volume is decreased by an order of magnitude.

The pseudospark operates on the left-hand-side of Paschen's curve, which shows the scaling of the breakdown voltage as a function of pd, where p is the gas pressure and d is the anode-cathode gap distance. Due to the special geometry of the pseudospark, the electric field distribution is non-uniform and time-dependent, resulting in a breakdown voltage that is shown to scale[8] as a function of $p^2 d$, although other scaling exponents have also been suggested[9]. Pseudospark discharges are operated just below the self-breakdown voltage and are externally triggered[10-14] by the injection of seed electrons into the hollow cathode cavity, which can be achieved electronically or by photo-emission. The optically-triggered method is usually referred to as the backlighted-thyratron (BLT). Experiments have shown that the number[10] of seed electrons needed to initiate a discharge is of the order of 10^9 to 10^{10}. For avalanche ionization, the ideal average energy of electrically triggered seed electrons should

be at the value corresponding approximately to the peak of the ionization cross-section[11], as examined later in the paper.

The physics of pseudospark operation can be complex and several characteristic phases have been identified by various authors. Although the nomenclature of such phases can be varied, it is generally agreed[15-17] that the discharge is characterized by space-charge build-up, followed by rapid ionization avalanche and electron beam formation, and finally a super-emissive state. The physical model for the latter phase (also called "super-dense glow") is not yet well understood, albeit likely to involve a self-sustained sputtering[18], and is not being modeled here; our attention is focused on the triggering and avalanche processes, which can be identified here as the (a) pre-breakdown and; b) breakdown phase. During the pre-breakdown phase electrons generated through ionization are accelerated to the anode leaving behind a region of net positive charge called the virtual anode. In the breakdown phase the plasma generation rate inside the virtual anode multiplies resulting in high plasma densities and the slow growth of the virtual anode. It is during this phase that an electron beam forms along the axis.

Temporal studies[4] of the time-to-breakdown have demonstrated a dependence on the trigger position, initial charge density and cathode face thickness. It was shown that the time to breakdown decreases when the trigger is moved closer to the cathode hole and increases with the initial seed charge density and thickness of the hollow cathode electrode.

In this article we report on the investigation of the variation of the magnitude of the electron peak current arriving at the anode with the hollow cathode dimensions and average electron seed energy using kinetic simulations. It is shown that all these factors combined affect the pre-breakdown and breakdown phases during the discharge development producing varying magnitudes of the peak electron current. In all the models studied the importance of secondary electrons due to both electron and ion impact of the surfaces on the discharge

development is also examined. In section II a description of the physical models employed in the study and the code used to generate the simulations, OOPIC Pro, is presented. The results of the simulations are discussed in section III, and conclusions are offered in section IV.

II. MODEL DESCRIPTION

The current investigation is performed through the analysis of two-dimensional electrostatic kinetic particle-in-cell (PIC) simulations generated by OOPIC-Pro[19], a well-validated software developed at Tech-X Corp. and capable of modeling both cartesian and cylindrical geometries. The code accounts for elastic and ionizing collisions using a Monte-Carlo procedure (MCC) and features both electrostatic and electromagnetic field solvers. The ionization model uses a cross-section model that is in very close agreement with the data from Phelps's tables[20]; only electron-impact ionization is being modeled. Additionally, secondary electrons from both electron and ion impact on the surfaces are modeled. OOPIC Pro employs a Vaughan based electron induced secondary emission model[22] that accounts for the angle of incidence and the energy dependence of the yield. Secondary electron emission due to ion impact employs a constant secondary coefficient of the value 0.1. Parameters used for both the electron and ion induced secondary electron models assume Molybdenum electrodes with a stainless steel cavity. The simulation parameters such as the cell-size, time-step and particle-weights have been selected to minimize the impact of fluctuations and grid heating. Each parameter has been decreased to a point where successive reductions produce the same physical results and the largest values with consistent outcomes have been selected to minimize computing time.

The physical model framework and geometry are illustrated in Figure 1. The pseudospark model has a fixed hollow cavity height Y_{max} = 50 mm and anode-cathode gap d_{ca} = 5 mm. The cathode thickness (w), depth (D), and hole height (h), are varied. The seed

electrons are injected near the back-wall of the hollow-cathode (see Figure 1), and various cases of energy are considered: (1) a directed velocity (along the $\hat{x}$-axis, towards the cathode hole) corresponding to a kinetic energy of 1 keV with a temperature of 2.5 eV (2) a directed mean kinetic energy corresponding to the peak of ionization cross-section; (3) no directed velocity, but a thermal distribution with a temperature of 2.5 eV which minimizes the number of electrons in the tail of the velocity distribution that have energies above the ionization threshold. These three cases correspond to high-, medium- and low-energy conditions for the seed electrons.

In all cases the discharge is filled with Argon gas at room temperature (300 ^{o}K) and at a pressure of approximately 0.44 torr (60 Pa), with an anode voltage is 10 kV and a grounded cathode. The approximate ionization mean-free-path at peak of cross-section is therefore $\lambda_i \approx 2.6\,\text{mm}$. Although this is smaller than the cathode-anode gap, the pressure was chosen such that the system is on the left-hand-side of Paschen's curve, since $pd_{ca} \approx 0.22\,\text{torr–cm}$, as illustrated in Figure 2. To distinguish the effect of secondary electrons from electron and ion impact to the surfaces, some simulation runs were performed with and without secondary emission. The total number of seed electrons is held constant at a value of 10^{11}; however, the rate of injection and overall injection time of the seed electrons is varied. In the high-energy case, i.e. when seed electrons are injected with an average energy of 1 keV, the injection period lasts for one nanosecond, while for the thermally emitted electrons, it ranges from 10 up to 1000 ns until a self-sustaining discharge is achieved (see sections III.A and III.B).

III. Computational Results and Analysis

Regardless of the variation in factors such as the hollow cathode dimensions and energy of seed electrons in the various cases studied, the general discharge development remains the same. First, the electric field due to the potential difference across the anode-cathode gap

penetrates into the hollow cathode, the extent of which being dependent on the hollow cathode dimensions. This electric field accelerates electrons to ionizing energies, generating an avalanche. At some location in the vicinity of the hollow cathode hole, depending on the geometry employed, the magnitude of the voltage drop is sufficient to accelerate the electrons out of the ionizing region to the anode, at a faster rate than the slower electrons upstream can replenish them, leaving a net positive space charge behind. In time, this positive charge region grows, distorting the field such that it extends further upstream into the hollow cathode expanding the ionizing region (see Figure 3). As the charge builds up, the electrostatic potential increases, forming a virtual anode that typically extends into the hollow cathode (see Figure 4), decreasing the potential difference across the anode-cathode gap[a)]. During that time the electron density and anode current increase, until the potential difference across the gap approaches a few percent of its initial value and the peak current is achieved.

For a given electron seed energy, the length of time taken to reach the breakdown phase is found to increase along with the hollow cathode thickness w, in agreement with the study by Pitchford *et al.*[4] on the temporal variation of the discharge with the hollow cathode dimensions and source location. Furthermore, it is found that the time taken to reach breakdown increases with the cathode depth D and decreases with the hole height h, for a given seed energy.

III.A. HIGH-ENERGY SEED ELECTRONS

When the seed electrons are injected with a mean velocity corresponding to a 1 kV kinetic energy, the peak current at the anode increases with the depth and thickness of the hollow cathode (see Figure 5). The cathode hole height h is 8mm and the hollow cathode thickness w and depth D range between 0.75 – 18.5 mm and 8 – 35 mm, respectively. Since the seed electrons have energies well above the ionization threshold they are able to create a

plasma as they move to the anode, as illustrated in Figure 6. As the net positive charge grows on the axis in the vicinity of the hollow cathode entrance and the electric field penetrates further upstream, the plasma initiated by the seed electrons provides an ample electron source, increasing the plasma generation rate and rapidly replenishing those electrons downstream that have left the region for the anode. As a result, a relatively large ion density (see Figure 7) fills the cathode bore region. If the hollow cathode depth is increased, a larger volume of plasma upstream of the hole can contribute to the current and increase its value. When the thickness of the hollow cathode is increased, the sheath still penetrates through the hole and into the backspace, forming a virtual anode in that region, as shown in Figure 8. Because this process takes longer as the thickness increases, the additional time available to electrons for building-up a plasma and the larger bore volume results in a larger peak current.

At the time of the peak electron current there are 0.72% of pendulum electrons at the ionization peak energy inside the hollow cathode cavity as Figure 9 illustrates. The pendulum electrons are defined as those with velocities in the $\hat{y}$ direction resulting in a kinetic energy around the peak ionization and a velocity in the $\hat{x}$ direction small enough to prevent the electrons from leaving this region during the time to breakdown.

Electron-impact secondary electron emission is too small for the current geometry to affect the discharge significantly during the time scales involved; therefore the value of the peak current remains approximately the same whether secondary electrons are included in the simulations or not.

III.B. Low-Energy Seed Electrons

Injecting seed electrons with a temperature of 2.5 eV without a mean velocity results in an electron peak current with a magnitude dependant primarily on the distance between the

electron source and the location of the electric field sufficient to accelerate the electrons to ionizing energies (see Figure 10). As in the previous energy case, we have $h = 8$ mm, $w = [0.75 - 18.5]$ mm, and $D = [8 - 35]$ mm. At the highest value of the peak current ($w = 0.75$ mm, $D = 18.5$ mm), the voltage drop sufficient to accelerate electrons to ionizing energies is located in front of the electron source. As before, the electrons start the avalanche process from the source as they move to the anode; decreasing the cathode depth results in a decrease in the peak current since this results in a smaller volume available to the electrons in which to create a plasma. For larger values of the hollow cathode depth and thickness the increase in distance between the electron source and the ionizing region results in a corresponding decrease in the peak current because, as the arrival rate to this region falls relative to the exit rate to the anode, the particle density decreases for a given net positive charge. The avalanche process can proceed only when the electric field is sufficient to accelerate electrons in the backspace and bore regions to ionization energy, as shown in Figure 11. Upstream of the ionizing region there is little plasma to rapidly replace the electrons lost to the anode and enhance the plasma generation rate, compared to the previous case of high-energy (1 keV) seed electrons. As a consequence, the charged particle densities are lower (compare Figure 12 with 7). As time progresses, the virtual anode still builds up and extends into the bore and hollow cathode a virtual anode that extends through the hole into the hollow cathode. However, for a given net positive charge density the electron density is much lower than for the high-energy case, a smaller peak electron current is generated. At the time of the peak electron current there are 0.64% pendulum electrons. The total number of pendulum electrons is 98% less than in the previous high-energy case.

Ion impact secondary electrons are more evident than the high-energy seed case for longer *w* because it takes $\approx$1000 ns as opposed to 13.3 ns for the virtual anode and the plasma to grow upstream through the hole during which time the interaction area slowly

increases and ions in these area's have more time to travel to the surface and interact. While secondary electron emission due to ion impact is too insignificant to affect the discharge in all the circumstances modeled there is a correlation between the yield and the impact surface area of the hole and the time taken to reach the peak current for the circumstances presented.

III.C. Medium-Energy Seed Electrons

In this case, the initial electrons are injected with a mean velocity corresponding to a kinetic energy equal to the ionization peak. This results in a peak electron current (see Figure 13) that depends both upon the time taken to reach this peak current and the distance between the electron source and the magnitude of the electric field sufficient to accelerate the electrons to ionizing energies (same as thermal/low-energy case). The number of electrons near the injection region is larger than in the thermal case, but due to large energy losses during ionizing collisions, most of the electrons in transit towards the anode have energies lower than the ionization threshold and are unable to generate any plasma until they regain kinetic energy from the voltage drop near the virtual anode (see Figures 14 and 15). This situation is similar to the previously examined case of low-energy. However, once the virtual anode extends into the hollow cathode and nears the seeding region, the plasma at that location provides a high density source of electrons and the beam current grows rapidly. In general, for a given depth and thickness, the magnitude of the peak current is smaller than the high-energy case, but larger than in the low-energy (thermal) case, due to the additional electron particle source that grows in front of the trigger which enhances the plasma generation rate during the breakdown phase.

Again, similar to what is found for thermally injected electrons, the magnitude of the peak electron current increases at a depth of D = 18.5 mm and thickness w = 0.75 mm since the initial penetrating electric field extends to the source increasing the avalanche rate in the

pre-breakdown phase (see section III.B). However, the greatest peak current occurs for the largest dimensions employed since the timescales allow more surplus plasma generation in front of the source.

III.E. Other Effects

The effect of the cathode bore height is examined in the high-energy case by reducing it to $h = 4$ mm (i.e. half the original size). There is a substantial increase in the peak anode current observed for the dimensions employed, where w = 0.75 and 8 mm and D =8 – 35 mm (see Figure 16). The trends in the peak current arriving at the anode with the hollow cathode depth and thickness are generally similar to that produced employing a hole height of 8mm except for larger values of both the thickness and depth.

It is more difficult for the electrons to enter a smaller hole, and the development of the virtual anode is delayed (see Figure 17). This gives more time for a plasma to build-up in the backspace region and provide a higher density source of electrons when the virtual anode finally reaches the edge of the plasma.

Figure 19 shows that for a cathode thickness of 8mm the peak current decreases as the depth increases above D = 18.5 mm; this can be tentatively explained as follows. The plasma is immediately generated by the 1 keV seed electrons starting from the source location, and as scattering events disperse the electrons as they travel downstream, the resulting peak in the plasma density is slightly downstream of the source. Eventually, when the space-charge field does penetrate the hollow cathode backspace these electrons in front of the source contribute to plasma generation and the peak density shifts downstream to close vicinity of the cathode hole entrance (see Figure 18). For the largest value of the peak current measured for $D = 18.5$ mm the electrons do not spread very far from the axis as they travel downstream and the virtual anode is able to penetrate far enough upstream to utilize most of these electrons.

When the depth increases to $D = 25 - 35$ mm, the seed electrons experience many more scattering events as they travel downstream, resulting in a much broader spreading pattern around the axis. Eventually, when the virtual anode extends into the hollow cathode backspace a substantial portion of the electrons previously generated in the interior are out of reach, resulting in smaller plasma generation rate near the hole where the electrons ultimately contribute to the peak current.

From Figure 16, one can also estimate that the electron-impact secondary emission contributes approximately 15% of the peak anode current. In this case of a smaller cathode hole, there is more interaction with surfaces on the backside of the hollow cathode face generating a greater number of secondary electrons to participate in the avalanche process. Thus, the effect of secondary emission is even smaller for larger cathode holes. The secondary electron yield decreases as a function of the electron impact energy for values less than that corresponding to the peak emission of 375 eV for Molybdenum and 400 eV for stainless steel. Therefore, it is expected that secondary electron emission will not affect the peak electron current for the other mean seed injection velocities employed in the study.

IV. CONCLUSIONS AND SUMMARY

We have examined the initial phases of operation of a transient discharge of a pseudospark type through electro-static PIC simulations; the computations were run until breakdown was achieved and a peak current from the electron beam was measured; the super-dense glow phase of operation was not examined. The magnitude of the peak current at the anode and time to breakdown (as measured by the time to reach this peak current) are examined as function of the geometrical parameters of the discharge, and for three cases of seed electron energy. The location of the seed electron injection was not varied, and the applied voltage was also held steady during operation.

The magnitude of the peak anode current is shown to have a complex dependence on the hollow cathode dimensions and the mean seed electron energy. This inter-dependence is achieved through the rate of growth of a plasma inside the hollow cathode, location of the peak density of this plasma, and the rate of penetration of a virtual anode through the cathode bore hole and into the backspace of the hollow cathode.

For the case of seed electrons at high-energy (many times the ionization peak value), plasma generation occurs independently of the rate at which the virtual anode penetrates into the hollow cathode. Thus the peak current has a very weak dependence on the discharge dimensions. The exception is at low values of both depth and thickness, as shown in Figure 5; a probable explanation is that in this case the high energy of the seed electrons is not effectively utilized, since they are absorbed by a wall before many ionization events could be realized. Assuming that the seed electron looses approximately half its kinetic energy through an inelastic collision with an atom, it would take 4-5 such collisions until the seed electron energy drops below the range for large ionization cross-section; thus after $4-5\lambda_i$, or 13 mm of combined length (depth and thickness), the variation of the peak current with distances should start to saturate; this appears to be approximately verified in Figure 5.

When the seed electrons are injected thermally (low-energy case), the opposite situation occurs, i.e. plasma generation is completely contingent upon the penetration of the virtual anode into the hollow cathode, since only the corresponding voltage drop will provide sufficient energy to the seed electrons for an ionization avalanche. This is clearly evident in Figure 11. In this case the larger the area within the hollow cathode backspace penetrated by the electric field, the greater the region over which particle multiplication can occur before the electrons are accelerated to the anode increasing the peak current. For the largest bore hole thickness, w =18.5 mm the electric field initially penetrates just the tip of the hole and then grows upstream to the hollow cathode interior. As the depth grows, the transit time of

the seed electron from the source to the plasma generation region increases compared to the time for electrons to leave this region for the anode; this results in a smaller electron density for a given net positive charge and a decrease in the peak electron current. This alternate dependency results in a different trend of the peak current with the hollow cathode dimensions. Seed injection at the intermediate energy of the ionization peak results in a discharge that is characterized by a combination of all three factors producing peak current trends that include features seen in the thermal and relatively fast seed injection cases.

The magnitude of the peak electron current arriving at the anode increases with the mean injection energy of the seed electrons for the values employed. Values above that required for ionization result in the generation of a surplus plasma independent of the electric field that penetrates the hollow cathode interior. Due to ionization energy losses, the magnitude of the surplus plasma generated, and the area covered, increases for the largest seed injection velocity used. This plasma acts as an additional particle source as the space charge distorted electric field grows upstream enhancing the plasma generation rate. The location of the growth of the additional plasma is also a factor, as is demonstrated when the hole height is decreased by half and seed electrons are injected with a mean energy of fifteen times the ionization peak. The obstruction caused by the decreased hole height results in a retardation of the growth of the space-charge distorted electric field, which increases the time over which surplus plasma generation occurs, resulting in larger peak electron currents for a given geometry. A trend of decreasing peak current as the hollow cathode size increases is observed for the largest dimensions employed. This trend is a result of the surplus plasma density peak being located in front of the source which becomes too remote to contribute.

Secondary electrons influence the discharge characteristics when the interaction area of the impacting species and the bombardment time are substantial. For all the geometries and mean seed injection velocities employed the ion impact secondary electron yield is too

insignificant to affect the discharge properties. However, secondary electrons resulting from electron impact are found to be influential on the magnitude of the peak current when the hole height is decreased in half and seed electrons are injected with a mean energy of fifteen times the ionization peak. In this system, the smaller hole results in a larger interaction area at the back side of the hollow cathode face and a longer discharge time. While the study examines the case of a reduced hole height for seed electrons with mean injection velocities corresponding to fifteen times the peak ionization energy exclusively, because of the energy dependence of the electron impact secondary yield it is expected that the magnitude of the peak current will not be affected by secondaries for the other mean seed injection velocities used.

The general discharge dependencies presented in this study are applicable to all gas types although argon, exclusively, has been employed in the investigation. While differences in the magnitude of the peak electron current and the amount of secondary electrons emitted which are attributable to the variation in the ionization cross-sections and ion mass are expected, similar trends with the mean seed injection energy relative to the ionization threshold should be generated.

ACKNOWLEDGEMENTS

This work was supported by an SBIR grant by the Office of the Secretary of Defense (OSD), contract #FA8650-04-C-2511.

Footnotes:

[a)] This penetration of the sheath into the hollow-cathode region has been simulated earlier[21] through different methods. However, the numerical approach of[21] uses a ballistic approximation for the electrons; the present work is a true PIC simulation that reproduces the time-scale of electron propagation.

REFERENCES:

[1] Rupert Tkotz et al, IEEE Trans. Plasma Sci. **23**, 309 (1995)

[2] Peter Choi et al, IEEE Trans. Plasma Sci. **17**, 770 (1989)

[3] K. Frank et al, IEEE Trans. Plasma Sci. **16**, 317 (1988)

[4] L.C. Pitchford et al, J. Appl. Phys. **78 ,** 77 (1995)

[5] Michael Gastel, Heike Hillmann, Ferdinand Muller and Jochen Westheide, IEEE Trans. Plasma Sci. **23**, 248 (1995)

[6] K. Frank and J. Christiansen, IEEE Trans. Plasma Sci. **17**, 748 (1989)

[7] Chunqi Jiang, Andras Kuthi and Martin A. Gunderson, Appl. Phys. Lett. **86** , 024105 (2005)

[8] K.K. Jain, B.N. Ding and M.J. Rhee, IEEE Particle Accelerator Conference (San Francisco, California, May 6-9, 1991)

[9] K. Frank et al., IEEE Trans. Plasma Sci. **27**, 1008 (1999).

[10] Thomas Mehr et al, IEEE Trans. Plasma Sci. **23**, 324 (1995)

[11] Marcus Iberler et al, IEEE Trans. Plasma Sci. **32**, 208 (2004)

[12] M. Legentil, C. Postel, J. C. Thomaz Jr. and V. Puech, IEEE Trans. Plasma Sci. **23**, 330 (1995)

[13] Yu. D. Korolev et al, IEEE Trans. Plasma Sci. **29**, 324 (2001)

[14] Harish K. Dwivedi, Jurgen Urban, and Klaus Frank, IEEE Trans. Plasma Sci. **30**, 1371 (2002)

[15] D. Bloess et al, Nucl. Instrum. Methods **205**, 173 (1983)

[16] Marcelo Zambra et al, IEEE Trans. Plasma Sci. **32**, 221 (2004)

[17] Bin Lin and Quantie Chow, IEEE Trans. Plasma Sci. **23**, 239 (1995)

[18] A. Anders et al., IEEE Trans. Plasma Sci. 23, 275 (1995).

[19] J.P. Verboncoeur, A.B. Langden and N.T. Gladd, Computer Physics Communications, **87**, 199 (1995)

[20] A.V. Phelps, jilawww.colorado.edu/www/research/colldata.html

[21] J.-P. Boeuf and L. C. Pitchford, IEEE Trans. Plasma Sci. **19**, 286 (1991)

[22] R. M. Vaughan, IEEE Trans. Electron Devices **40**, 1963 (1993)

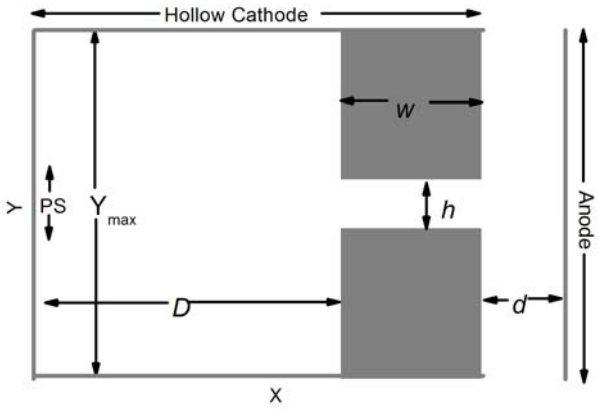

Figure 1

FIG. 1: Problem configuration, where PS indicates the electron seed injection location.

Figure 2

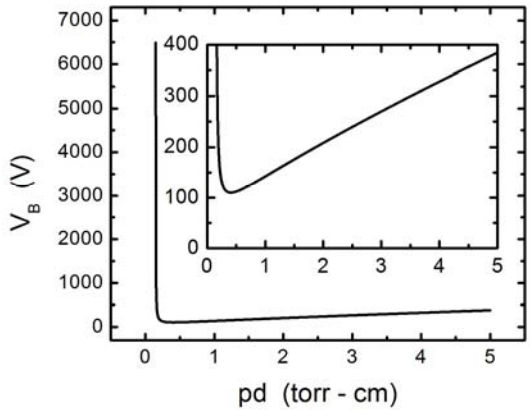

FIG. 2. Paschen's curve for argon, where p = pressure, d = anode –cathode gap, V_B = breakdown voltage and the minimum is at pd = 0.4 torr – cm.

Figure 3

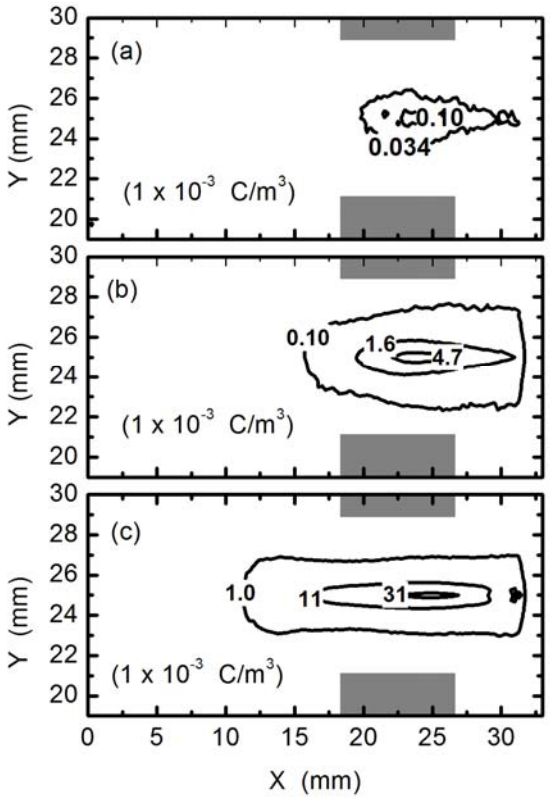

FIG. 3. The net positive charge density for a hollow cathode depth D =18.5 mm, thickness w = 8 mm, hole height h =8 mm, at the times (a) 30ns (b) 55 ns and (c) 63.6 ns, where the electron peak current is achieved at 63.6 ns. The gray boxes indicate the hollow cathode face.

Figure 4

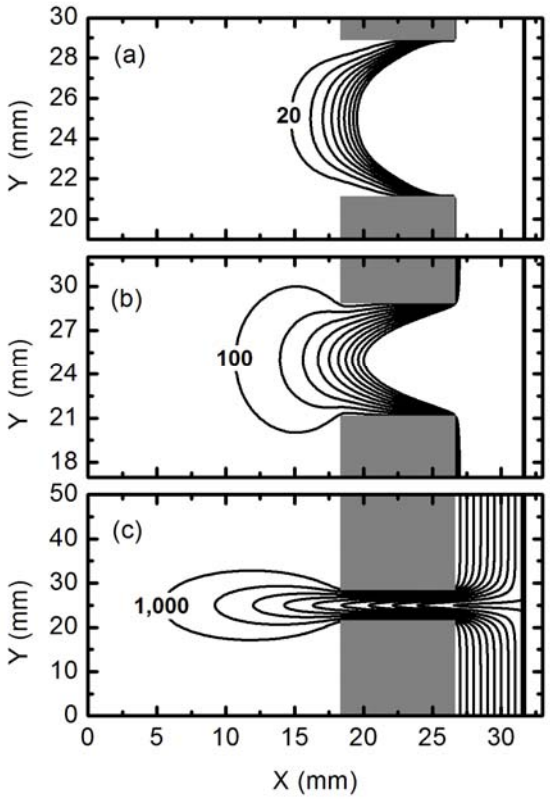

FIG. 4. The electrostatic equipotential contours for a hollow cathode depth D =18.5 mm, thickness w = 8 mm, hole height h =8 mm, where illustrated are the first ten contours with (a) 20 V spacing at the time 30ns (b) 100 V spacing at the time 55 ns and (c) 1000V spacing contours at the time 63.6 ns. The electron peak current is achieved at 63.6 ns. The gray boxes indicate the hollow cathode face.

Figure 5

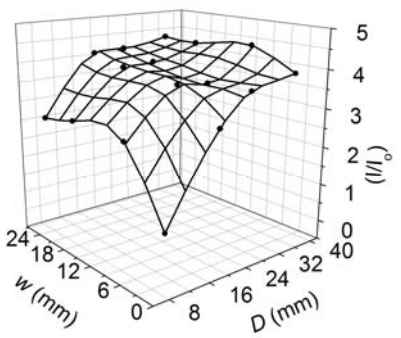

FIG. 5**.** The variation in the peak electron current arriving at the anode with the hollow cathode depth, D, and thickness, w, where I_o is the peak current for D = 8mm, w =0.75mm, h= 8mm and 1 keV seed electrons, the hole height h =8 mm and the seed electrons are injected with a mean velocity corresponding to a 1kV acceleration. The grid is a best fit to the data.

Figure 6

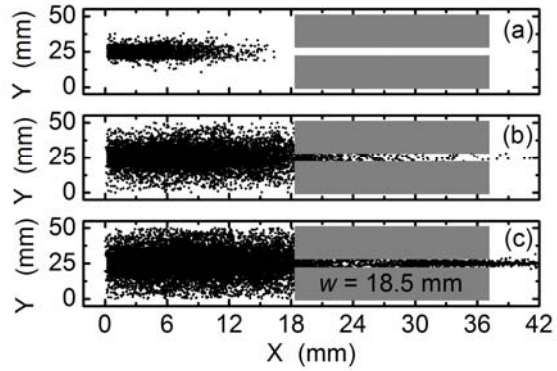

FIG. 6. Argon ion X -Y space for a hollow cathode depth D = 18.5 mm and hole height h = 8mm and the seed electrons are injected with a mean velocity corresponding to a 1kV acceleration for the times (a) 1 ns (b) 3 ns and (c) 5 ns, where the electron peak current is achieved at 16 ns.

Figure 7

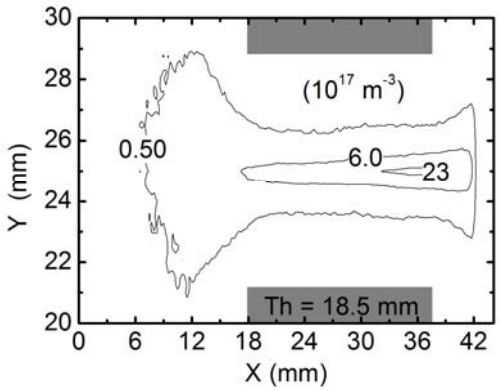

FIG. 7. Argon ion density for a hollow cathode depth D = 18.5 mm, hole height h = 8mm and the seed electrons are injected with a mean velocity corresponding to a 1kV acceleration at the time when the electron peak current is achieved at 16 ns.

Figure 8

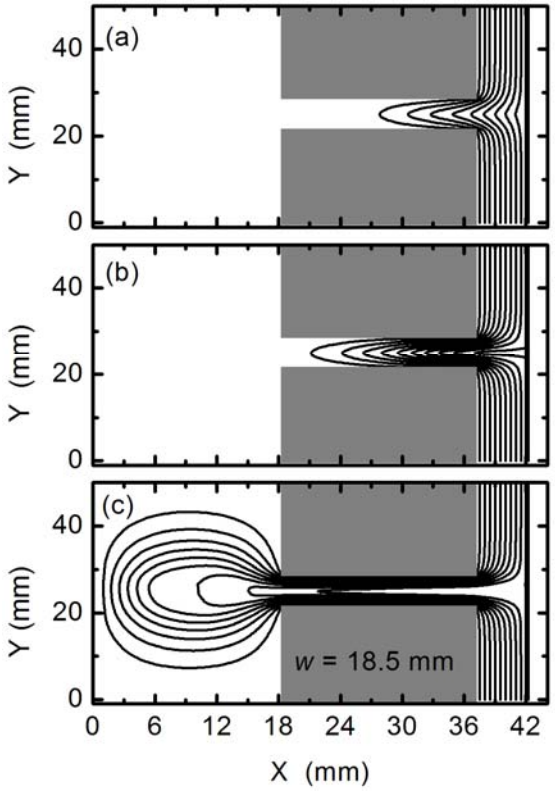

FIG. 8. The electrostatic equipotential contours with a 1kV spacing for depth D = 18.5 mm, hole height h = 8mm and the seed electrons are injected with a mean velocity corresponding to a 1kV acceleration for the times (a) 10 ns (b) 13 ns and (c) 16 ns, where the electron peak current is achieved at 16 ns.

Figure 9

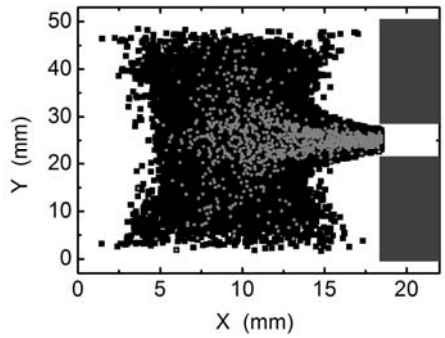

FIG. 9. Electron velocities in the cathode hollow cavity (a) and (b) and (c) X – Y space of the pendulum electrons (gray) and all electrons (black), where D = 18.5 mm, w = 18.5 mm and the seed electrons are injected with an average energy of 1 keV. The gray boxes indicate the hollow cathode face.

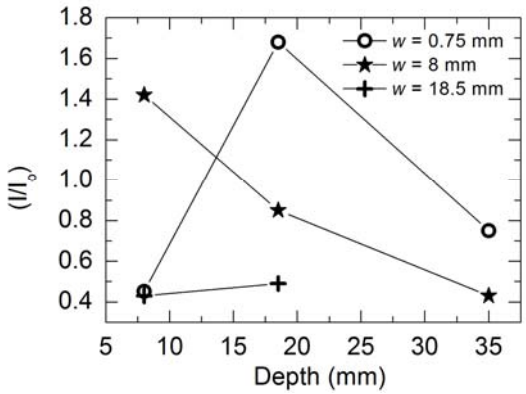

Figure 10

FIG. 10. The variation in the peak electron current arriving at the anode with the hollow cathode depth, *D*, and thickness, *w*, where I_o is the peak current for *D* = 8mm, *w* =0.75mm, *h*= 8mm and 1 keV seed electrons, the hole height *h* =8 mm and the seed electrons are injected energies up to 2.5 eV.

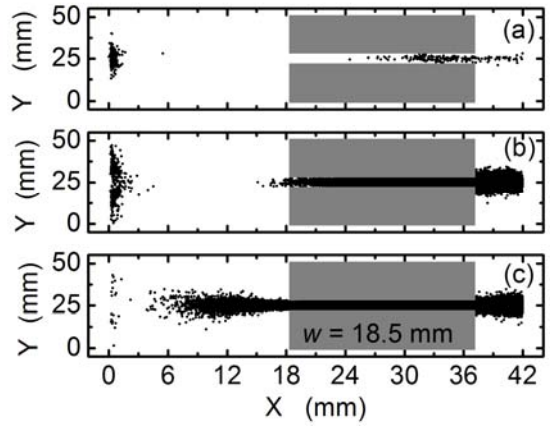

Figure 11

FIG. 11. Argon X - Y phase space for a hollow cathode depth *D* = 18.5 mm, hole height *h* = 8mm and the seed electrons are injected with energies up to 2.5 eV for the times (a) 64 ns (b) 930 ns and (c) 1016 ns, where the electron peak current is achieved at 1017 ns.

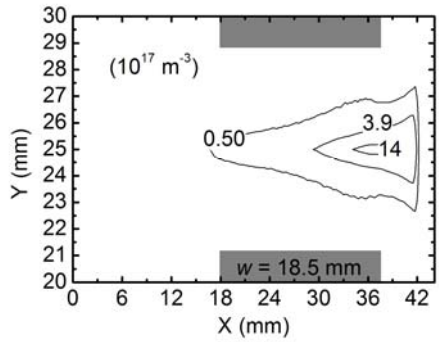

Figure 12

FIG. 12. Argon ion density for a hollow cathode depth *D* = 18.5 mm, hole height *h* = 8mm and the seed electrons are injected with energies up to 2.5 eV at the time 1016 ns, where the electron peak current is achieved at 1017 ns.

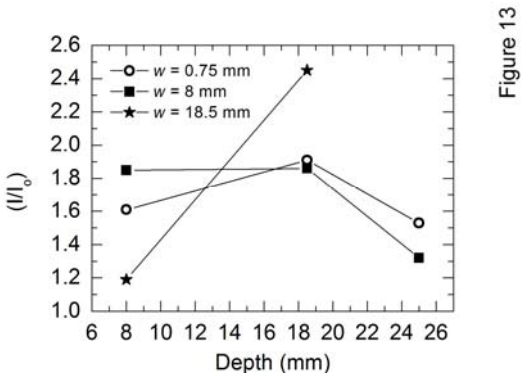

FIG. 13. The variation in the peak electron current arriving at the anode with the hollow cathode depth, *D*, and thickness, *w*, , where I_o is the peak current for *D* = 8mm, *w* =0.75mm, *h*= 8mm and 1 keV seed electrons, the hole height *h* =8 mm and the seed electrons are injected with an average energy equal to the ionization peak.

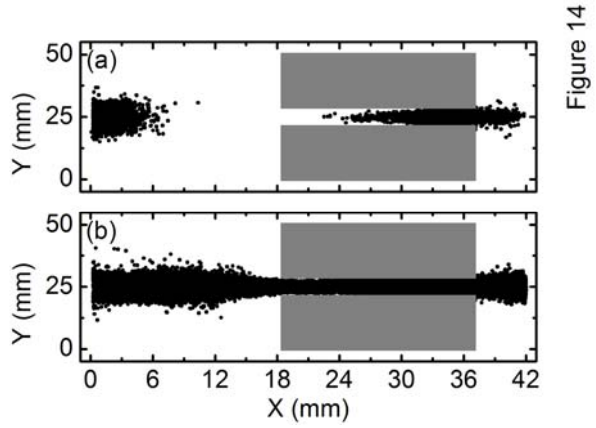

FIG. 14. Argon X - Y phase space for a hollow cathode depth *D* = 18.5 mm, hole height *h* = 8mm and the seed electrons are injected with an average energy equal to the ionization peak for the times (a) 25 ns and (b) 38.5 ns, where the electron peak current is achieved at 38.5 ns. The gray boxes indicate the hollow cathode face.

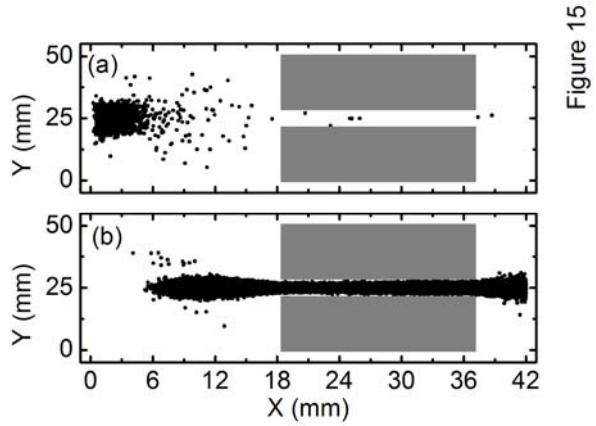

FIG. 15. Electron X - Y phase space for a hollow cathode depth *D* = 18.5 mm, hole height *h* = 8mm and the seed electrons are injected with an average energy equal to the ionization peak for the times (a) 25 ns and (b) 38.5 ns, where the electron peak current is achieved at 38.5 ns. The gray boxes indicate the hollow cathode face.

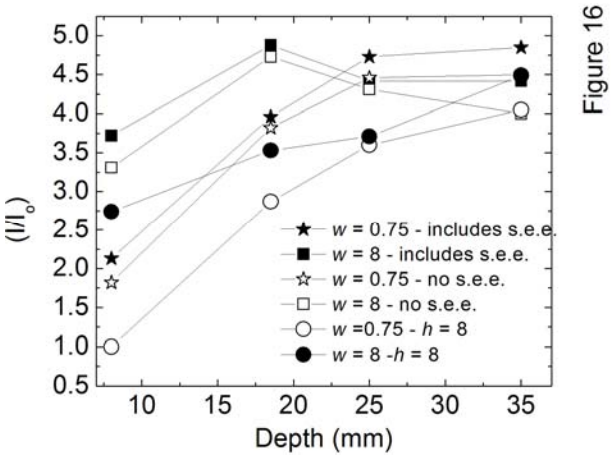

FIG. 16. The variation in the peak electron current arriving at the anode with the hollow cathode depth, *D*, and thickness, *w*, where I_o is the peak current for *D* = 8mm, *w* =0.75mm, *h*= 8mm and 1 keV seed electrons, the hole height *h* =4 mm, unless otherwise stated, sizes are in mm, and the seed electrons are injected with a mean velocity corresponding to a 1kV acceleration.

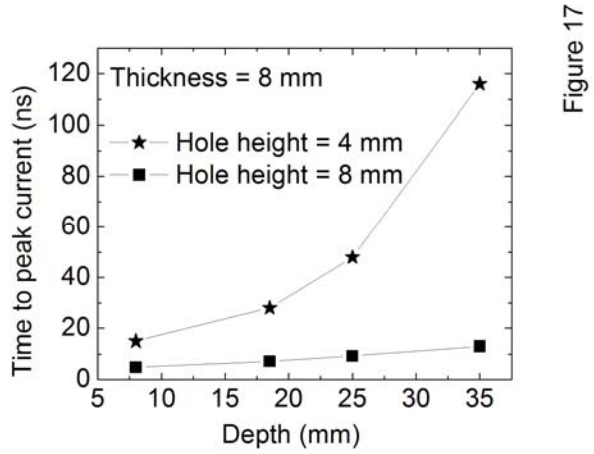

FIG. 17. The time taken to reach the peak current for a given hollow cathode depth, where seed electrons with an average energy of 1 keV are employed.

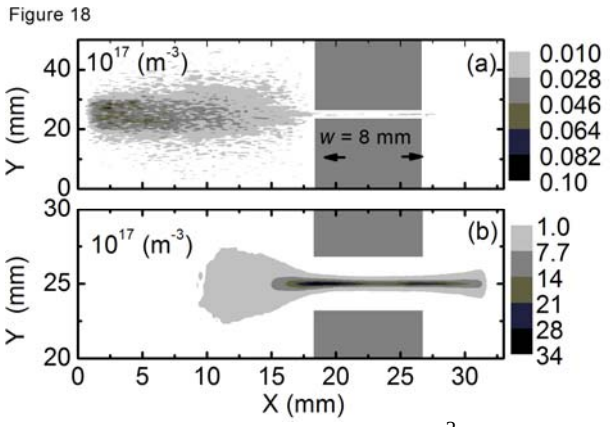

FIG. 18. The electron density (m^{-3}) for a hollow cathode depth *D* =18.5 mm, hole height *h* = 4mm and the seed electrons are injected with a mean velocity corresponding to a 1kV acceleration at the times (a) 11 ns and (b) the time of the peak current 28.6 ns.